



Ex-Post Evaluation of Countermeasures Against Residual Settlement of an Ultra-Soft Peaty Ground Due to Test Embankment Loading: A Case Study in Maizuru-Wakasa Expressway in Japan

Mutsumi Tashiro, Lecturer, Institute of Innovation for Future Society, Nagoya University (Nagoya, Japan); email: mutsumi@civil.nagoya-u.ac.jp

Minoru Kawaida, Managing Executive Officer, Traffic and Environment Research Department, Nippon Expressway Research Institute Company Limited (Tokyo, Japan); email: m.kawaida.aa@ri-nexco.co.jp

Motohiro Inagaki, Manager, Gifu Construction Office, Central Nippon Expressway Company Limited (Gifu, Japan); email: m.inagaki.aa@c-nexco.co.jp

Shotaro Yamada, Associate Professor, Department of Civil and Environmental Engineering, Tohoku University (Sendai, Japan); email: shotaro.yamada.d2@tohoku.ac.jp

Toshihiro Noda, Professor, Disaster Mitigation Research Center, Nagoya University (Nagoya, Japan); email: noda@nagoya-u.jp

ABSTRACT: Before the construction of the Maizuru-Wakasa Expressway in Japan, a test embankment was constructed in 2006 on ultra-soft ground containing an approximately 50 m thick, soft peat layer with N -values of 0 to 1, and large-scale settlement over 11 m was observed within 4 years after loading. Numerical analyses were conducted by the authors to predict the future settlement and evaluate the effectiveness of countermeasures. The soil-water coupled finite deformation analysis code GEOASIA was used, employing an elastoplastic constitutive model, the SYS Cam-clay model, to describe the mechanical behavior of the soil skeleton structure. The simulation results were applied to the actual design of repair work performed on the test embankment. Furthermore, in the subsequent embankment construction, the countermeasures were implemented taking future maintenance into consideration. This study conducts ex-post evaluations of the countermeasures against residual settlement based on the valuable monitoring data for 6 years from the start of the expressway operation. It also shares how the design principles for the residual settlement of soft ground have changed throughout Japan's highway construction history, including in this case.

KEYWORDS: residual settlement, soft ground, embankment loading, clay, peat, soil structure, SYS Cam-clay model, soil-water coupled analysis, ex-post evaluation

SITE LOCATION: [Geographic Database](#)

INTRODUCTION

Construction of embankments on soft ground requires close attention to stability during loading and residual settlement afterward. Embankments for expressways must typically be higher to allow for multi-level crossings with local streets. Depending on the type and state of the soft ground on which they are constructed, such embankments can cause considerable deformation resulting in long-lasting, far-reaching effects.

Since the former Japan Highway Public Corporation (current NEXCO) first began constructing expressways in Japan in 1958, instances of soft ground have been encountered in approximately 50 regions around the country. Although expressway design and construction in the early years relied heavily on technology and knowhow from Europe and the U.S., as Japanese

Submitted: 12 January 2021; Published: 10 December 2021

Reference: Tashiro M., Kawaida M., Inagaki M., Yamada S., and Noda T. (2021). Ex-Post Evaluation of Countermeasures Against Residual Settlement of an Ultra-Soft Peaty Ground Due to Test Embankment Loading: A Case Study in Maizuru-Wakasa Expressway in Japan. International Journal of Geoengineering Case Histories, Volume 7, Issue 1, pp. 58-75, doi: 10.4417/IJGCH-07-01-03

engineers gained experience through domestic construction, they accumulated knowledge from domestic measurements and the development of new technologies the field has led to the development of home-grown design principles specific to Japan. In this paper, we first examine how design principles for dealing with large long-term settlements of soft ground have changed over the course of Japan's expressway construction history. Next, we report on a case involving embankment construction on ultra-soft peaty ground that represents the first application of the concept of "soil structure" proposed by Mikasa (1962) to the actual planning of expressway embankments in Japan, and which marks a major turning point in design principles. According to Mikasa, the mechanical properties of soil are determined by the type and condition of the soil. Then, factors other than the density and water content that define the condition are collectively defined as the soil skeleton structure. For saturated soil, the density and water content are synonymous, so the difference in mechanical behavior between artificially remolded soil and naturally deposited soil is due to the degree of soil structure development. The results of the authors' numerical analysis-based research were applied to the actual construction plan at this site, leading to the proactive implementation of novel countermeasures against residual settlement. Finally, we discuss the results of ex-post evaluations of countermeasures deployed at the site to deal with residual settlement of peaty ground based on predictions from numerical analysis and in-situ measurements.

To provide context to this study, we begin in the next section by examining the current state of large long-term settlement in the context of expressway construction in Japan and the design principles previously applied to such construction. Next, we introduce previous numerical analysis-based studies carried out by the authors related to the large long-term settlement of soft clayey ground. As part of this discussion, we outline a new theory of soil mechanics underlying numerical analysis, that is the mechanisms of large-scale, long-term settlement due to the structural failure of clayey soil.

We then introduce case studies in which results of the authors' previous research were applied to the actual planning of an embankment constructed on ultra-soft peaty ground. The Mukasa area of the Maizuru-Wakasa Expressway, the construction of which was completed in July of 2014, comprises ultra-soft peaty ground that is highly uncommon even in Japan. The ground contains a peat layer with N -values ranging from 0 to 1 and a soft clayey layer with a maximum thickness of approximately 50 m, as shown in Figure 1. Four years after the start of test embankment construction in February 2006, the total settlement had reached 11 m. On-site investigations and laboratory experiments revealed that the more-than-30-m deep peat layer, which, at the design stage, was believed would not contribute to settlement, was, in fact, undergoing substantial compression and that further settlement was expected to occur. Applying the results of our research on the large long-term settlement of soft clayey soil to the site conditions, we were able to reproduce the observed large-scale settlement caused by the test embankment and to predict future residual settlement. In addition, we performed numerical analyses to evaluate the effectiveness of various countermeasures against the residual settlement of peaty ground: slow-rate banking, lightweight banking, and ground improvement through vertical drains or vacuum consolidation. The results of this research were applied to large-scale repair work performed on a test embankment as well as to countermeasures against residual settlement that were implemented in the construction of subsequent embankments in the same area.

In this study, we performed ex-post evaluations of countermeasures against the residual settlement of peaty ground deployed at the site based on six years' worth of settlement data and records of maintenance and repair work since the expressway entered service in 2014. Two ex-post evaluations are reported: the evaluation for lightweight banking implemented on a test embankment located at point STA 498+25, and the evaluation for vertical drain/vacuum consolidation on an embankment at point STA 501+20 constructed after the test embankment was completed. Based on the experience at this site, methods proposed by the authors have been incorporated as standard practice in the July 2015 revision of the NEXCO design standards. We introduce principles for dealing with large long-term settlement that are incorporated in the latest version of the design standards and summarize the main findings of this study.

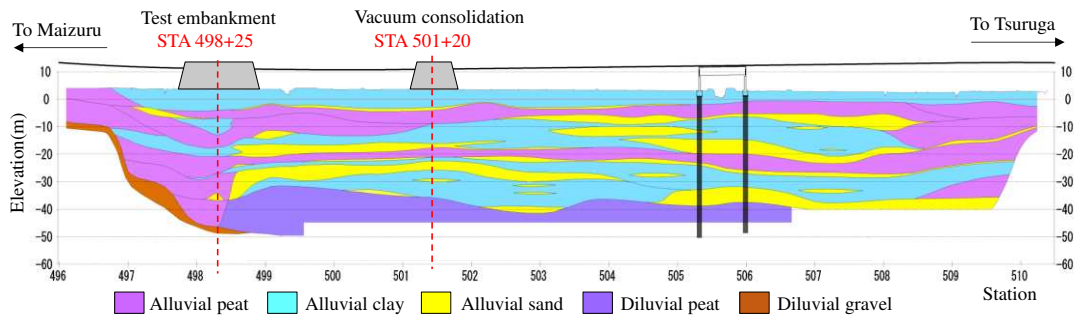


Figure 1. Soil strata in the Mukasa area (longitudinal section).

BACKGROUND

Evolution of Design Principles Related to Countermeasures Against Residual Settlement

Soft ground was encountered in the very first case of expressway construction in Japan—the Meishin Expressway—bringing to the fore the challenge of dealing with such ground. Designs and calculations were made based on the most up-to-date theory of soil mechanics at the time, and full-scale test embankments were constructed in some areas. Various methods such as surcharging, preloading, and the installation of vertical drains were proactively tested as possible countermeasures against settlement.

As field observation data began to accumulate for locations around the country, it became evident that settlement did not occur as predicted before construction. This led to a shift in practice towards predicting future settlement based on observed settlement during construction and as operation and maintenance proceeded. Although the vertical drain method was shown to be an effective ground-stabilization measure, it did not prove to be a successful countermeasure against residual settlement at that time. Furthermore, frequent repairs associated with residual settlement were necessary for about five years after highways entered into service and it was found that residual settlement could be taken care of with asphalt overlays. For this reason, design principles were revised in 1983, recommending that ground improvement not be performed at the time of construction as a countermeasure against residual settlement and, instead, to deal with residual settlement in the operation and maintenance stage by selecting road structures that account for residual settlement to reduce total costs.

Expressways were constructed on soft ground around the country based on these design principles, with follow-up surveys being carried out to evaluate the settlement in regions where residual settlement occurred. Data accumulated over a period of more than two decades revealed that residual settlement of 1 m or greater occurred after entry into service in approximately 20% of the 50 or so locations where soft ground was encountered. It was also found that substantial money and labor is being expended for maintenance and repair in these locations. In addition, long-term monitoring revealed new cases where settlement accelerated due to sand drains.

Figure 2 shows approximately twenty years' worth of settlement data for two test embankments in the Kanda area of the Joban Expressway (Noda et al., 2005). In this example, Embankment A, which was constructed on unimproved ground, is a preloaded site that has a history of reconstruction using tunnel muck after the removal of dredged sand. The ground under Embankment B was improved using sand drains that extended to a depth of 20 m. Although no differences between these two embankments can be seen in the early data, the long-term data clearly show that sand drains accelerated settlement. In the case of Embankment A, for which no ground improvement was carried out, settlement has continued over the long term, necessitating repeated repair using asphalt overlays. Sixteen years after entry into service, the residual settlement was 188 cm. This large long-term settlement has necessitated not only the repair of height differentials and slopes that have occurred on the embankment itself but repeated repair of surrounding fields and substantial expenditures for maintenance and repair. Estimating total design costs from construction to maintenance and repair requires an accurate prediction of settlement. However, it has not been possible to predict large long-term settlement of the type observed in the Kanda area, either based on soil mechanics theory or measurement data.

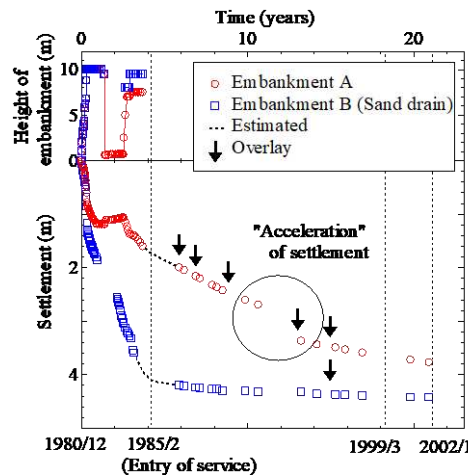


Figure 2. Long-term observed data in the Kanda area (Noda et al., 2005).

Over the same period, substantial data has been accumulated on the soil profile of soft ground in areas where expressways have been constructed. The 2005 revision of *Design Standards (Earthwork)* (Japan Highway Public Corporation, 2005) classified ground comprising soft layer (including loose sand) having a thickness of 15 m or greater as “deep-layer type (Type III)” ground and explicitly stated that such ground types are highly prone to large settlement. The document also introduced, as a new design principle, the possibility of using vertical drains as a countermeasure against long-term residual settlement when so indicated based on constructing test embankments. However, as the theory needed to assess the potential for large long-term settlement and the efficacy of vertical drains had not yet been established, it was difficult to incorporate vertical drains into designs.

Proposed Method for Simulating and Predicting Large Long-Term Settlement Caused by the Structural Decay in Clay

In Noda et al. (2005), the authors used numerical analysis to simulate the large long-term settlement observed in the Kanda area and to explain the underlying mechanism. Naturally-deposited clays generally have a higher void ratio and exhibit greater consolidation yield stress than remolded clay, which results in the loss of strength and substantial compression upon disturbance. The elasto-plastic constitutive equation SYS Cam-clay Model (Asaoka et al., 2002) describes this as a phenomenon accompanying structural degradation caused by the plastic deformation of highly structured (bulky) soils. Using this equation, we were able to explain the mechanism of long-term settlement as a soil-water coupled finite deformation problem wherein long-term settlement results from the delayed dissipation of excess pore water pressure caused by progressive structural degradation/failure within the soft clay layer. Other phenomena besides long-term settlement that cannot be explained by the conventional elastic/elasto-plastic consolidation theory have also been observed in the Kanda area, including the acceleration of settlement under constant loading and increased excess pore water pressure in the soft clay layer. In the above study, we were also able to demonstrate that these phenomena can be reproduced as soil-water coupled phenomena associated with soil skeleton structure failure.

Having established that the concept of “soil structure” is critical to the problem of large long-term settlement, we proposed a simple method for determining the types of sites where large residual settlement is likely to occur (Inagaki et al., 2010) with the ultimate goal of applying the results of the above study to actual embankment design. We examined an array of field data and laboratory test results on naturally-deposited clay identified as being the cause of settlement for multiple sites where expressway embankments have been constructed on soft ground. The study revealed that predicting residual settlement magnitude requires not only an assessment of embankment load and soft clay layer thickness but also an evaluation of the mechanical characteristics of the soft clay based on laboratory tests. As can be seen in Fig. 3, we proposed “having a compression index ratio of 1.5 or higher and a sensitivity ratio of 8 or higher” as criteria for determining whether a naturally-deposited clay has the potential for large residual settlement. In this case, the compression index ratio was defined as the ratio of the steepest gradient of the compression curves for the undisturbed sample and for the remolded sample (Fig. 4).

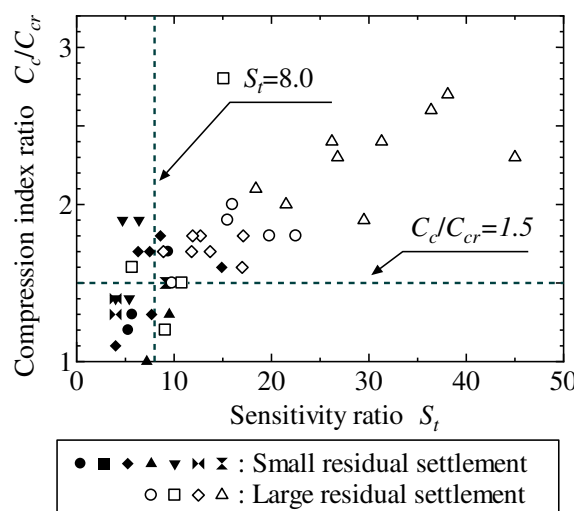


Figure 3. Classification based on the sensitivity and compression index ratio (Inagaki et al., 2010).

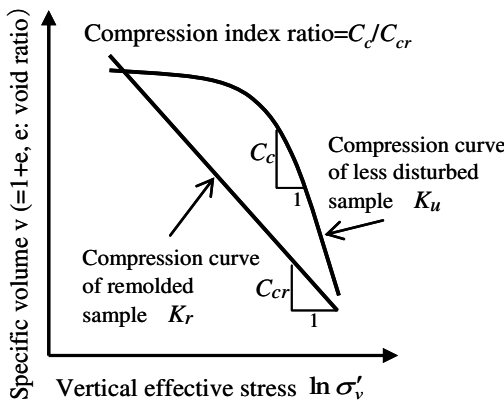


Figure 4. Definition of the compression index ratio (Inagaki et al., 2010).

Based on the SYS Cam-clay Model, clays with large sensitivity and compression index ratio can be described as soils that initially possess a high degree of structure, and decay of structure can occur easily due to plastic deformation. This type of clay tends to exhibit dramatic decreases in compressibility caused by disturbances that occur during field sampling, removal from the sampling tube, specimen preparation, and setting-up on the test apparatus. Accordingly, settlement greater than that predicted from compression curves for “undisturbed” samples may occur in-situ, leading to large residual settlement.

Within the scope of soils that we have investigated, the residual settlement observed in grounds consisting of clays with both a low sensitivity ratio and a low compression index ratio has been small and can be adequately predicted using existing forecasting methods based on the compression theory proposed by Terzaghi (1925). In contrast, the clay soil of the Kanda area described above has a high sensitivity ratio and a high compression index ratio, as shown by white square in Figure 3, and the actual settlement observed was approximately double the 2 m predicted prior to construction. In response, the authors proposed a novel method for predicting settlement for grounds that are likely to experience large residual settlement. With this method, settlement is predicted using the soil-water coupled finite deformation analysis code GEOASIA (Asaoka and Noda, 2007; Noda et al., 2008) after estimating the high compressibility of a soil in-situ from the compression curve for an undisturbed sample. Tashiro et al. (2011) applied the proposed method to sites where residual settlement is actually progressing and verified the method’s efficacy.

At the target site in Tashiro et al. (2011), residual settlement of 70 cm was observed by the fourth year after entry into service. Given the substantial excess pore water pressure remaining in the clay layer, it was predicted that further settlement would occur. From a simple criterion proposed by the authors, it was confirmed that the ground contained clayey soils that are sensitive to disturbance and have a possibility of large residual settlement. In our analysis, we reproduced the magnitude of settlement and pore water pressures observed up to the fourth year after the start of embankment construction. We used only the permeability coefficients for the soil layers as fitting parameters and predicted future settlement based on them. Figure 5 shows the simulation results and measurements reported in Tashiro et al. (2011) with the addition of observed settlement data for the ten or so years following the analysis (open red circles). The simulation demonstrated the high precision of the method proposed by our research group. The dotted line in Figure 5(b) indicates the predicted amount of final settlement calculated from the compression curves of undisturbed samples using the Δe method (2.1 m). It can be seen that settlements of more than twice the calculated value by the simple conventional method have occurred. The measurements indicated a slightly faster settlement than predicted, which is probably due to a cross-sectional repair.

EX-POST EVALUATION OF LIGHTWEIGHT BANKING FOR TEST EMBANKMENT

Prediction of Future Settlement and Assessment of Lightweight Banking

In this section, we summarize research reported in Tashiro et al. (2015), entailing the prediction of future settlement of a test embankment in the Mukasa area of the Maizuru-Wakasa Expressway (STA 498+25 in Fig. 1) and an assessment of lightweight banking as a countermeasure against residual settlement.

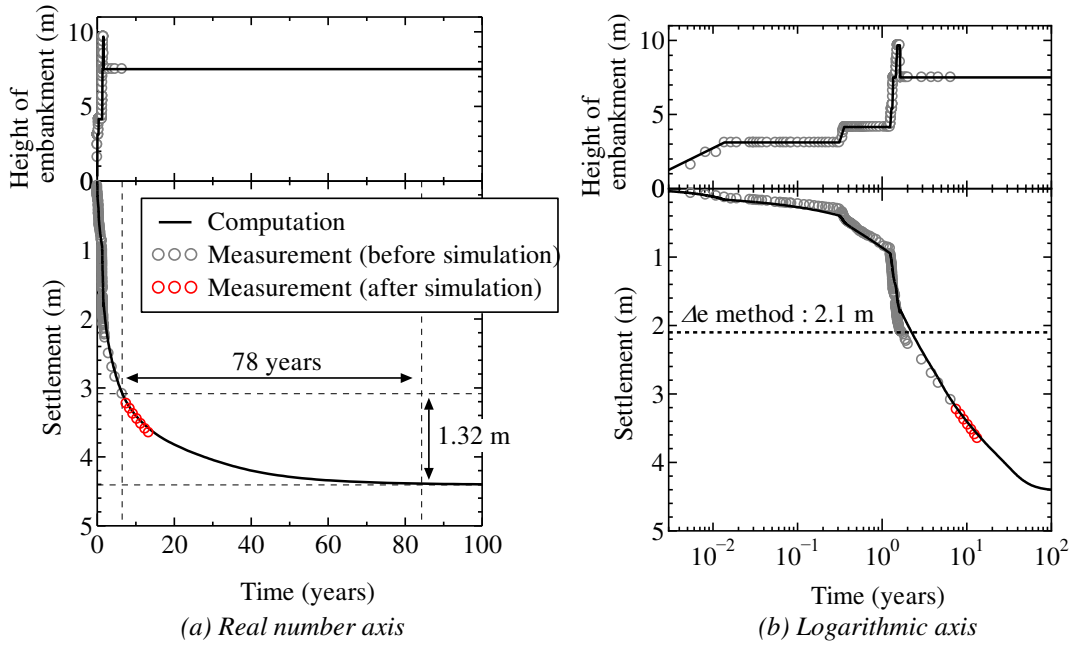


Figure 5. Ex-post evaluation of residual settlement prediction of soft clay ground (added to Tashiro *et al.* (2011)).

Construction of the Mukasa test embankment began in February 2006 for the purpose of assessing stabilization countermeasures and preloading the site for box culvert construction. As aforementioned, the maintenance and repair work needed to counter residual settlement associated with the construction of expressway embankments on soft clayey ground had, by that time, already become problematic around the country. Therefore, in the Mukasa area, the residual settlement was examined prior to construction. Because the soft ground layer in the Mukasa area, although thick, is mainly composed of peat with relatively high permeability, it was expected that the settlement that occurred in the shallow peat layer would converge approximately during construction. Based on practical experiences in similar peat grounds, it was also decided that the settlement caused by the deeper peat layers would be limited, and even if it lasted until after construction, it could be addressed by setting a sufficient period for the consolidation process and designing structures that accommodate settlement. Although ground improvement by the installation of vertical drains to a depth of 20 m was carried out, the purpose was not to prevent residual settlement but to ensure stability.

In reality, however, substantial settlement also occurred even in the deep peat layer (30 m and deeper) and, by the time the embankment design height of approximately 7 m was achieved, the embankment thickness (embankment height + settlement) was 17 m. An uplift of up to approximately 1 m and a horizontal displacement of approximately 2 m were observed near the toe of slope. Approximately four years after the start of embankment construction, the total settlement exceeded 11 m and was progressing at a rate of 4.0 cm/month with no indication of convergence.

Because the test embankment was constructed to cross a local road and a waterway, a section of the embankment was scheduled to be replaced with a box culvert before the expressway was put into service. If residual settlement occurs after box culvert installation, a differential settlement may occur between the box culvert and the surrounding embankment that will necessitate repair. However, because the box culvert was to be installed at a section where the number of lanes on expressway changes and traffic regulation would have been difficult, it was imperative that the frequent repair of differential settlement be avoided and the need for maintenance minimized. If the floor of a box culvert were to sink as a result of settlement, the box culvert's water channels would not function and substantial maintenance costs would be incurred to pump water up and out. For this reason, engineers were faced with the urgent challenge of predicting possible future residual settlement and identifying effective countermeasures against it.

A survey of the site conducted in October of 2009 revealed that, owing to the artesian pressure conditions of the valley bottom created through fault activity, the consolidation yield stress of the deep peat layer directly under the Mukasa test embankment was smaller than the effective stress predicted from the normal hydrostatic pressure distribution and that the peat layer was highly compressible. Except for this one characteristic, the ultra-soft peaty ground in the Mukasa area could be handled with

the same methodology used in previous research for soft clay soil (Tashiro et al., 2011). In other words, peat has a higher degree of structure than naturally-deposited clay and, because of this, can undergo rapid massive compression when the consolidation yield stress is exceeded. At the same time, because the permeability suddenly declines, dissipation of excess pore pressure is delayed, and settlement continues for a long time.

These features could be expressed by using the SYS Cam-clay model, which can describe the behavior of the soil skeleton, and the soil-water coupled finite deformation analysis code GEOASIA, which incorporates the model. In addition, we were able to reproduce the settlement of different layers observed up to March 2010 and to predict future residual settlement using the method proposed by our research group which had been validated for ground containing clays that are sensitive to disturbance and have a possibility of large residual settlement (described in the prior section). For greater detail on the analysis conditions, please see Tashiro et al. (2015).

Figure 6 shows the observed and simulated values for the soil directly under the center of the embankment. Simulating the magnitude of settlement yielded pore water pressures that closely matched observed values. If the end of consolidation is defined as the point in time when the settlement rate under the embankment center reaches 1 mm/year, it is estimated that additional settlement of 1.52 m will occur over approximately 66 years. The prediction of substantial residual settlement indicated that it would also be necessary to lighten the embankment in the vicinity of the box culvert to reduce differential settlement between the embankment and the box culvert.

To estimate the magnitude of residual settlement that would result from lightweight banking, we conducted further analyses using the GEOASIA code. For simplicity, lightweight banking was modeled by removing finite elements corresponding to the embankment. We instantly removed the embankment load four years after the start of embankment construction in the simulation shown in Fig. 6 and calculated the subsequent behavior. Results of this analysis are shown in Fig. 7. It was found that greater load reduction resulted in earlier convergence of settlement and less residual settlement. Based on this analysis, excess height was added to the box culvert cross-section during actual construction to accommodate residual settlement of up to 1.2 m, and a sinking allowance was incorporated by raising the initial vertical alignment. In addition, embankment material for a large area of the embankment, spanning approximately 50 m, was replaced with lightweight material. Figure 8 shows the test embankment after the implementation of lightweight banking.

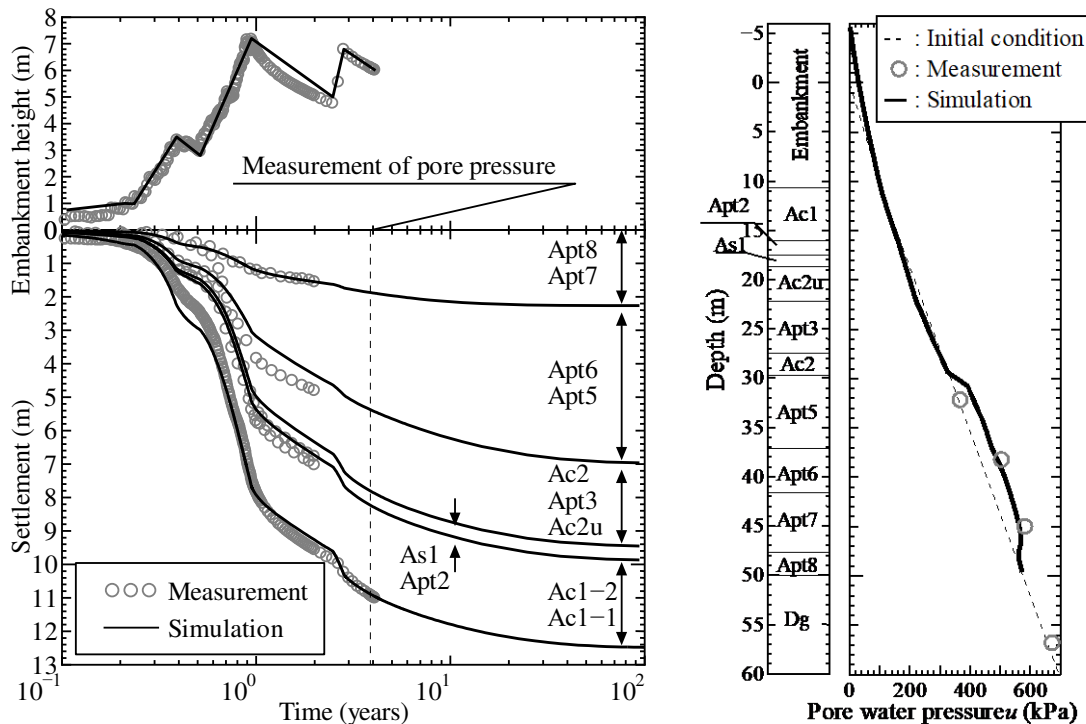


Figure 6. Simulation and predictions of large-scale settlement of the test embankment (STA 498+25, Tashiro et al., 2015).

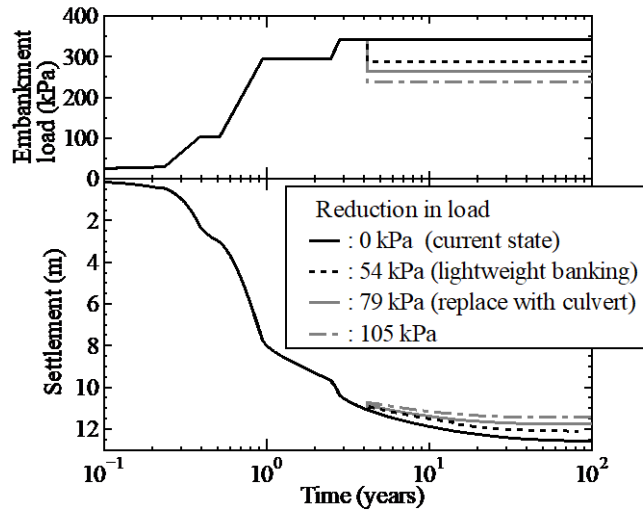


Figure 7. Effect of lightweight banking method (Tashiro et al., 2015).



Figure 8. Lightweight banking near culvert box (STA498, taken in 2013, Tashiro et al., 2015).

Ex-Post Evaluation of Lightweight Banking

Ground surface settlement measurements for the test embankment (STA 498+25) after box culvert replacement are shown by the red circles in Fig. 9. For comparison, the figure also shows simulated settlements for a load reduction of 54 kPa from Fig. 7 (black line). The settlement measurement point was changed from the ground surface to the crown of the embankment starting in 2014. Subsequent settlement magnitudes were compared assuming that the observed and simulated values were equal as of 2014. The “embankment height” provides a history of lightening of the embankment adjacent to the box culvert. Actual construction was carried out by removing part of the embankment and replacing it with a box culvert or a lightweight embankment with a rectangular cross-section. Because the timing and history of load removal differ, it is not possible to directly compare the simulated and observed results. However, the results indicate that lightweight banking is effective for early convergence and reduction of residual settlement. As of 2020, work to repair height differentials has not been performed once in the six years since the embankment was entered into service.

Revision of Principles for Countermeasures Against Residual Settlement Post-Test Embankment

In Tashiro et al. (2015), we also performed numerical analyses on slow banking and ground improvement by vertical drain installation. In the case of the Mukasa test embankment, the rate of embankment construction was controlled based on embankment height. However, rapid settlement during embankment construction necessitated an increase in the loading rate, which resulted in large-scale deformation of the ground near the embankment. The results of numerical analysis indicated that slowing construction would be effective in not only preventing deformation of the shallow ground layers but could also reduce residual settlement. Based on these findings, embankment since that test embankment has been constructed by

controlling embankment thickness rather than embankment height. In addition, in cases where sufficient construction time is not available, vacuum consolidation is carried out along with slow banking.

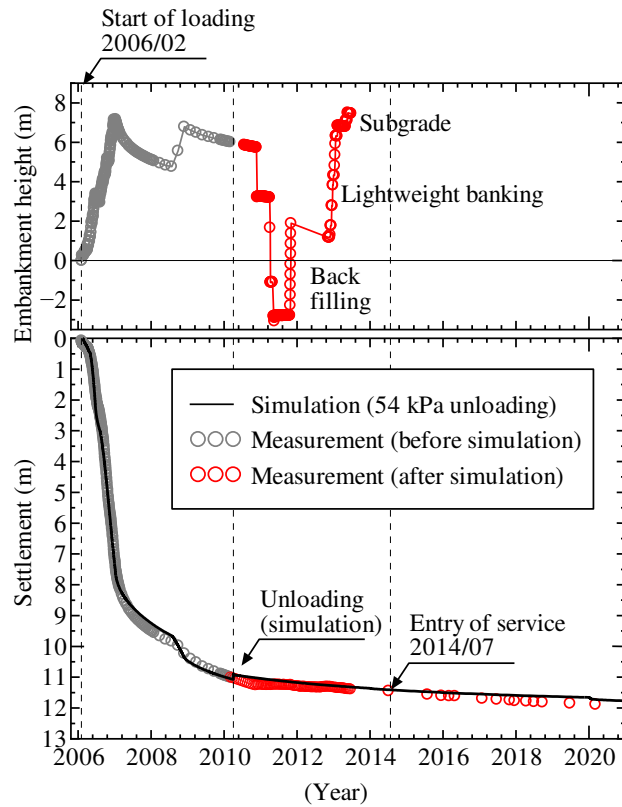


Figure 9. Ex-post evaluation of lightweight banking method for the test embankment (STA 498+25).

For the test embankment, vertical drains were installed to increase ground stability. The numerical analysis revealed that massive circular slip failure, including in deep soil layers, would have occurred if the vertical drains had not been installed and that the installation of vertical drains was effective in prevent catastrophic slip failure. The numerical analysis also indicated that expansion of the ground improvement area, both in breadth and depth, would reduce both total settlement and residual settlement. Based on the experiences of the test embankment and the results of our numerical analyses, the installation of vertical drains down to the deep soft layer has become a standard application as a countermeasure against residual settlement by embankment loading in the Mukasa area.

Given the magnitude of the settlement in peaty ground, the settlement cannot be completely eliminated even if the above-mentioned countermeasures against residual settlement are employed. For this reason, in the Mukasa area, countermeasures to prevent differential settlement between the embankment and structures such as bridges and box culverts were proactively deployed to reduce the need for maintenance and repair even if settlement occurred. These countermeasures included increasing both the “sinking allowance” section with preset high alignments and the “smoothing” section where the bridge abutment and the embankment are loosely connected by deep soil mixing. Thanks to the deployment of these countermeasures, repair work in the entire Mukasa area over the six years since entry of the expressway into service has been limited to a single case.

EX-POST EVALUATION OF VACUUM CONSOLIDATION/VERTICAL DRAINS

Simulations Based on a Newly-Proposed Macro-Element Method

In this section, we summarize our research as reported in Nguyen et al. (2015), which involved simulating the peaty ground underlying an embankment located approximately 300 m from the test embankment on the Tsuruga side (STA 501+20 in Fig. 1) that was subjected to vacuum consolidation starting from 2012. At this site, vacuum consolidation using an airtight

sheet (Association of Vacuum Consolidation Technology, 2013) was implemented to reduce construction time. Prefabricated Vertical drains (PVDs) using plastic board (100 mm in width and 7 mm in thickness) were installed to a depth of 20 m in a square pattern with drain spacing of 0.7 m. After one month of vacuum loading at approximately 60 kPa, the embankment was built up at a rate of approximately 8 cm/day until the final height of approximately 8 m was reached. Vacuum loading was continued for two months after the end of construction.

Site surveys and laboratory tests revealed that, unlike the ground underlying the test embankment at STA 498+25, the ground at site STA 501+20 was only minimally affected by artesian conditions and, therefore, the deep peat layers exhibited sufficiently large consolidation yield stress. It was also found that alternating clay and sand layers existed in the middle of the soil profile. That said, the shallow layers at the two sites were found to have very similar soil types and conditions insofar as neither was affected by artesian conditions. Based on this data, it was predicted that although the stability and settlement of shallow ground layers at site STA 501+20 may be problematic, large residual settlement of the type observed at the test embankment will not occur. At the same time, it was feared that the presence of middle sand layers spanning the entire improvement area might cause vacuum consolidation to affect surrounding areas. In fact, settlement up to 5 cm was observed after the start of vacuum consolidation over a wide area located approximately 50 m from the toe of the embankment slope.

In the analysis of the test embankment discussed in the previous section, the mass permeability of the ground, including vertical drains, was expressed using the mass permeability method (Asaoka et al., 1995), in which the mass permeability was back calculated based on observed data. This method, however, did not allow for the direct evaluation of the impact of vertical drain spacing, permeability, and the area that undergoes improvement. For this reason, we proposed a new macro-element method (Yamada et al., 2015, hereinafter the “newly-proposed macro-element method”), which adds water adsorption and discharge functions to the conventional macro-element method proposed by Sekiguchi et al. (1986). Thereupon, we applied the mass permeability, conventional macro-element, and newly-proposed macro-element methods to numerical analysis and evaluated the ability of each method to reproduce the observations at the STA 501+20 site.

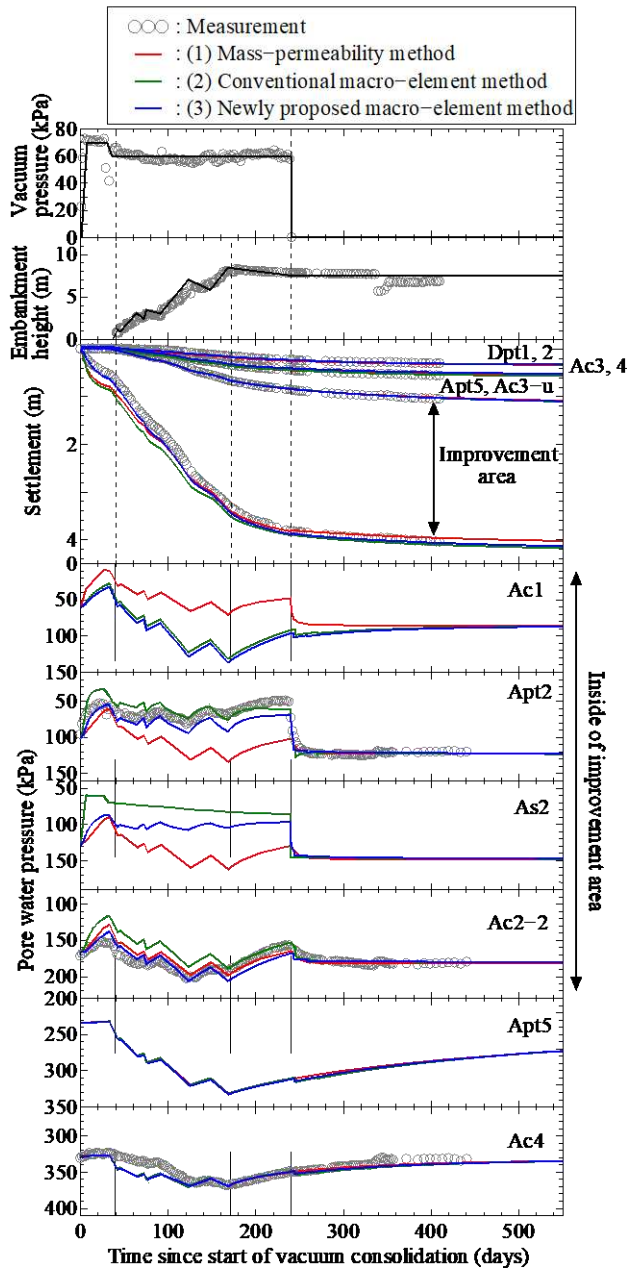
Results of simulations using these three methods are presented in Fig. 10. All the methods exhibited similar abilities to reproduce ground surface settlement. The analysis based on the mass permeability method overestimated the impact of vacuum consolidation on shallow ground layers in the improved area, underestimated the impact on deep ground layers, and was unable to reproduce the settlement over a wide area beyond the improved area. The newly-proposed macro-element developed by the authors was able to comprehensively and accurately simulate all types of observed ground behaviors.

In light of continuing the simulation into the future using the same parameters, it was predicted that consolidation of the ground improved by vertical drains would end early and that, although residual settlement would occur in deep layers that were not improved, the magnitude of this settlement would be small. In addition to the simulations described above, the authors evaluated the impact of vertical drain spacing using numerical analysis (Nguyen et al., 2015). It was found that the same residual settlement reduction achieved with vertical drains plus vacuum consolidation can be achieved using vertical drains alone if the spacing is appropriately close.

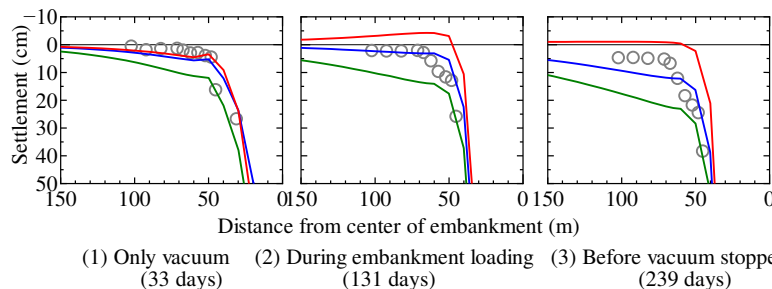
Ex-Post Evaluation of Ground Improvement via Vertical Drains and Vacuum Consolidation

Subsequent observed data for the site STA 501+20 are shown as red circles in Fig. 11. To enable a comparison, the horizontal axis is the same as that in Fig. 9. The simulated results, based on the newly-proposed macro-element method from Fig. 10, are shown with black lines. Simulated and observed values were assumed to be the same at the start of service. The observed values show that residual settlement ended later than predicted by the simulation. Possible reasons for this discrepancy include the fact that the simulation did not account for additional loading such as that due to paving or insufficient simulation accuracy owing to the scarcity of in-situ data for the target embankment compared to the test embankment.

Alternatively, it is possible that the inhibitory effect of vacuum consolidation on residual settlement was overestimated in the simulation. Figure 12 compares residual settlement at the site STA 501+20 (red line: PVDs + vacuum) and at a point located 40 m from the site where the ground was improved using only PVDs without vacuum consolidation (blue line: PVDs only). The ground profile and embankment loading history were essentially the same in both locations. These data indicated that, thanks to the presence of middle sand layers, no problems with stability occurred in the ground that was improved using only PVDs without vacuum consolidation and that the implementation of vacuum consolidation along with PVDs did not greatly reduce residual settlement. These observations closely match the results of the numerical analysis in Nguyen et al. (2015). It is speculated that ongoing residual settlement occurs in peat layers deeper than the improved area by vertical drains. It would have been better to install the vertical drains even deeper.



(a) Time-settlement / pore water pressures relations at the center of embankment



(b) Settlement of the surrounding ground

Figure 10. Reproduction analysis of improvement effects by vacuum consolidation and vertical drains.

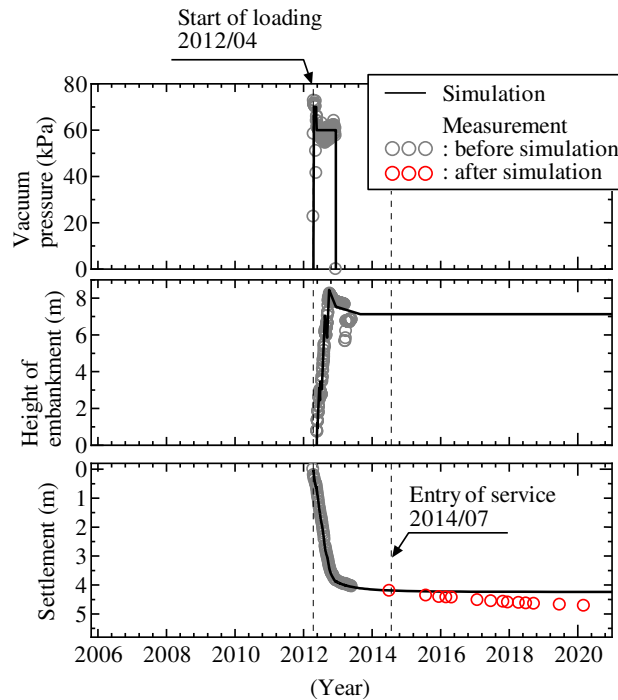


Figure 11. Ex-post evaluation of vacuum consolidation / vertical drains (STA 501+20).

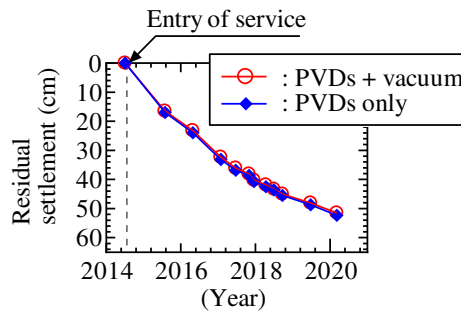


Figure 12. Comparison of residual settlement (measurements).

CONCLUDING REMARKS

The series of related studies by the authors introduced in this paper and the application of research results to the ultra-soft peat ground in the Mukasa area reconfirm the following:

- Large long-term settlement that cannot be predicted by conventional soil mechanics and observational methods occurs in soft ground depending on the type and condition of soils composed the ground.
- When large long-term settlement occurs, substantial labor and cost must be expended on maintenance and repair work.
- A new understanding of soil mechanics that accounts for soil skeleton structures and the disturbance is particularly significant in terms of being able to assess the potential for large long-term settlement and to predict future settlement.
- Ground improvement employing vertical drains is effective for ground that is predicted to undergo large long-term settlement.



The NEXCO Group's design standards, revised in July 2015, incorporate the above points related to large long-term settlement. The following is a summary of these standards.

- Determine the potential for large long-term settlement based on the thickness of the soft layer that is subject to settlement as well as the sensitivity ratio and compression index ratio of the soils constituting the soft layer.
- For ground predicted to undergo large long-term settlement, perform ground improvement at the time of construction by employing vertical drains or other countermeasures to proactively accelerate settlement.
- For designing the improved area and the spacing of vertical drains, construct a test embankment and estimate residual settlement after entry into service using a finite element analysis method that has been demonstrated to be effective.
- Choose embankment and structures that will require minimal maintenance and repair even if residual settlement occurs.

It is also worth noting that settlement forecasting based on a finite element analysis was introduced to the revised design standards as a method for supporting overall decision-making at the practical planning stage. The current approach to planning based on observed values is limited in terms of its ability to predict residual settlement and evaluate the impact of countermeasures for sites with complex loading histories, such as lightweight banking after preloading on the test embankment. The fact that we were able to propose a new method as a result of repeated trial and error at field sites for the purpose of truth-seeking based on numerical analysis is highly meaningful. We hope to continue similar investigations in the future.

In addition, the design standards specify that settlement forecasting for ground where large long-term settlement is expected should be carried out based on a soil-water coupled finite element analysis with an elasto-plastic constitutive equation capable of describing the behavior of the soil skeleton structure—in other words, the GEOASIA-based method proposed by the authors. GEOASIA can describe not only clay and peat but all soil materials (from sand to embankment material) within the same theoretical framework. Furthermore, the creation of formulas based on an equation of motion that accounts for inertial forces enables continuous handling of not only large long-term settlement behavior but everything up to instantaneous circular slip failure. These characteristics allow researchers to comprehensively evaluate the efficacy of countermeasures against various phenomena that occur in the field.

The Mukasa area of the Maizuru-Wakasa Expressway represents the first application of new design principles that are not beholden to past approaches to design. The field observation data collected so far and the state of maintenance and repair confirm the appropriateness of these design principles and demonstrate a dramatic reduction in road maintenance costs. That said, given the possibility that phenomena exceeding our current predictions will occur in the future, we will continue to carefully monitor the results of field observation.

ACKNOWLEDGMENTS

Special thanks to all the people involved NEXCO (formerly JH) for providing us with valuable field data.

APPENDIX

A1. The Super/Subloading Yield Surface (SYS) Cam-clay Model (Asaoka et al., 2002; Noda et al., 2009)

Quantified expression of structure, overconsolidation, anisotropy, and their respective evolution rules

Naturally deposited soils, whether clayey or sandy, generally exist in a structured and overconsolidated state. For example, in the case of clay, structured clay occupies a greater bulk than the remolded clay, that is, structured clay can take its mechanical state in “Impossible Region (Atkinson and Bransby, 1978)” for the remolded clay (e.g., Fig. A1). To describe the deformation behavior of a soil in this state, we must start from the base of an elasto-plastic model of an unstructured soil in a state of normal consolidation. Given that a soil in this unstructured and normally consolidated state still possesses anisotropy, the method presented in this paper is based on the modified Cam-clay model of Roscoe and Burland (1968), with the introduction of the rotational hardening concept of Sekiguchi and Ohta (1977), which treats the stress parameter η^* and its evolution rule as an expression of anisotropy. The degrees of structure and overconsolidation are then introduced and quantified by means of two concepts: the superloading surface for structure (Asaoka et al., 1998b; Asaoka et al., 2000; Asaoka

et al., 2002), and the subloading surface for overconsolidation (Hashiguchi, 1978; Hashiguchi, 1989; Asaoka et al., 1997). That is to say, the degree of structure is expressed by means of a superloading surface situated on the outside of the Cam-clay normal-yield surface and similar to it, with the center of similarity being the origin $p' = q = 0$ and the similarity rate being given by R^* , where $(0 < R^* \leq 1)$. At the same time, the overconsolidation state is expressed by means of a subloading surface situated on the inside of the superloading surface and again similar to it, with the center of similarity $p' = q = 0$; the similarity rate R , where $(0 < R \leq 1)$; and the reciprocal $1/R$ is the overconsolidation ratio. In this formulation, p' is the mean effective stress, and q is the deviator stress. Using the effective stress tensor \mathbf{T}' (tension: positive): $p' = -\text{tr} \mathbf{T}'/3$, $q = \sqrt{3/2 \mathbf{S} \cdot \mathbf{S}}$.

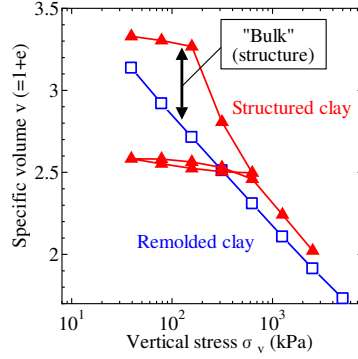


Figure A1. Typical oedometer test results on structured clay and remolded clay (Noda et al., 2005).

The closer R^* is to 0, the higher the degree of structure. However, as progressive plastic deformation induces a loss of structure, R^* will approach 1, which is the evolution rule for R^* . Similarly, the closer R is to 0, the more overconsolidated the state of the soil; as R increases toward 1 with plastic deformation, the state of the soil will also approach normal consolidation, which is the evolution rule for R . Therefore, the loss of structure induced by progressive plastic deformation can be assumed to induce a simultaneous release from overconsolidation and a transition to the normally consolidated state, finally resulting in conditions that match those in the Cam-clay model. The relative positions of the three loading surfaces, assuming conditions of axial symmetry, are as shown in Fig. A2.

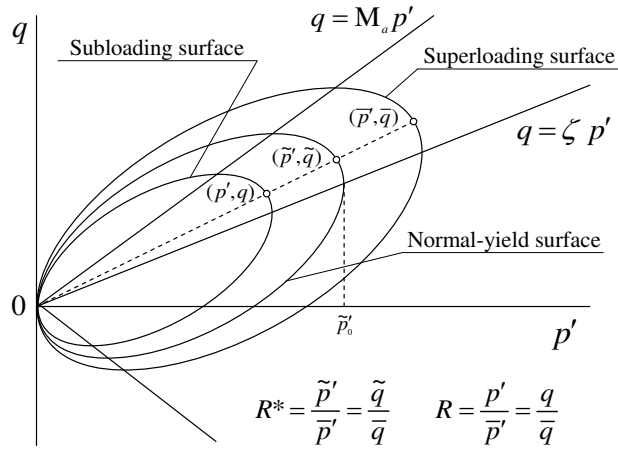


Figure A2. Three loading surfaces.

Based on the Cam-clay potential represented by Eq. (A1) below, and given that the current effective stress exists on the subloading surface, we first derive Eq. (A2) to adapt relations to the subloading surface through the application of various elasto-plastic principles such as the associated flow rule and Prager's consistency condition.

$$\text{MD} \ln \frac{\tilde{p}'}{\tilde{p}_0} + \text{MD} \ln \frac{M^2 + \eta^*{}^2}{M^2} + \int_0^t \text{Jtr} \mathbf{D}^p d\tau = f(\tilde{p}', \eta^*) + \int_0^t \text{Jtr} \mathbf{D}^p d\tau = 0 \quad (\text{A1})$$

$$f(p', \eta^*) + MD \ln R^* - MD \ln R + \int_0^t J \text{tr} \mathbf{D}^p d\tau = 0 \quad (A2)$$

Here, $D = (\tilde{\lambda} - \tilde{\kappa})/M/(1 + e_0)$ is the dilatancy coefficient; M , $\tilde{\lambda}$, $\tilde{\kappa}$, and e_0 are the critical state constant, compression index, swelling index, and initial void ratio, respectively; $J = (1 + e)/(1 + e_0)$, where e is the void ratio at time $t = t$; and $-\int_0^t J \text{tr} \mathbf{D}^p d\tau$ (compression: positive) corresponds to the plastic volumetric strain. The expression of anisotropy is obtained using the rotational hardening variable β , where $\beta = \mathbf{0}$ expresses a state of no anisotropy, from the calculation $\eta^* = \sqrt{3/2 \hat{\eta} \cdot \hat{\eta}}$; $\hat{\eta} = \eta - \beta$; $\eta = \mathbf{S}/p'$; and $\mathbf{S} = \mathbf{T}' + p' \mathbf{I}$. In the present paper, the evolution rules for R^* , R , and β are given by the following equations.

$$\text{Evolution rule for } R^* : \dot{R}^* = J \sqrt{\frac{2}{3}} \|\mathbf{D}_s^p\|, \quad U^* = \frac{a}{D} R^{*b} (1 - R^*)^c \quad (A3)$$

$$\text{Evolution rule for } R : \dot{R} = J U \|\mathbf{D}^p\|, \quad U = -\frac{m}{D} \ln R \quad (A4)$$

$$\text{Evolution rule for } \beta : \dot{\beta} = J \frac{br}{D} \sqrt{\frac{2}{3}} \|\mathbf{D}_s^p\| \|\hat{\eta}\| \left(m_b \frac{\hat{\eta}}{\|\hat{\eta}\|} - \beta \right) \quad (A5)$$

Here, \mathbf{D}^p is the plastic stretching tensor, \mathbf{D}_s^p is the deviator component of \mathbf{D}^p , and $\|\mathbf{A}\|$ represents the norm of a tensor \mathbf{A} . In Eq. (A5), $\dot{\beta}$ is Green and Nagdhi (1965)'s rate of β . The parameter groups for the evolution rules in Eqs. (A3) – (A5) all consist of constants, and from their respective functions, we may call a , b , and c the degradation indices of structure; m the degradation index of overconsolidation; br the rotational hardening index; and m_b the rotational hardening limit constant.

Associated flow rule and constitutive equation:

$$\text{Associated flow rule} : \mathbf{D}^p = \lambda \frac{\partial f}{\partial \mathbf{T}'}, \quad \lambda = \frac{\frac{\partial f}{\partial \mathbf{T}'} \mathbf{T}'}{J \frac{MD}{p'(M^2 + \eta^{*2})} (M_s^2 - \eta^2)} > 0 \quad (A6)$$

$$\text{Constitutive equation} : \dot{\mathbf{T}'} = \mathbf{E} \mathbf{D} - \Lambda \mathbf{E} \frac{\partial f}{\partial \mathbf{T}'} \quad (A7)$$

Here, \mathbf{E} is the elastic modulus tensor, $\dot{\mathbf{T}'}$ is Green and Naghdi's rate of \mathbf{T}' , and Λ is the expression of the plastic multiplier λ in terms of stretching \mathbf{D} . Further, we can establish the relations

$$M_s^2 = M_a^2 + br \frac{4M\eta^{*2}}{M^2 + \eta^{*2}} (m_b \eta^* - \sqrt{\frac{3}{2}} \hat{\eta} \cdot \beta) - MD \left(\frac{U^*}{R^*} 2\eta^* + \frac{U}{R} \sqrt{6\eta^{*2} + \frac{1}{3} (M_a^2 - \eta^2)^2} \right) \quad (A8)$$

and

$$M_a^2 = M^2 + \zeta^2, \quad \zeta = \sqrt{3/2} \|\beta\| \quad (A9)$$

The slope M_s of the threshold between hardening and softening $q = M_s p'$, obtained under loading conditions $\lambda > 0$, varies according to structural degradation, loss of overconsolidation, and development or loss of anisotropy, as well as with the current stress ratio. Similarly, the slope M_a of the threshold between plastic compression and expansion $q = M_a p'$ varies in response to the development or loss of anisotropy. For details, the reader is referred to Asaoka et al. (2002).

A2. GEOASIA (All Soils All States All Round Geo-Analysis Integration) (Noda et al., 2009)

Governing equations of soil skeleton-pore water coupled finite deformation analysis

We here explain the governing equations for finite deformation fields, including the rate-type equation of motion for saturated soils (Asaoka and Noda, 2007; Noda et al., 2008). The details of the formulation and the solution method are shown in Noda et al. (2008). Based on the two-phase theory of mixtures, we consider the soil skeleton and pore water to be the constituent phases of the mixture, and formulate the respective equations for these solid and fluid phases. The governing equations shown below are based on $u-p$ formulation. To carry out a finite deformation analysis using updated Lagrangian, which takes into

consideration the continuously changing geometrical shape of the saturated soil (mixtures), rate-type equations of motion are allotted to the saturated soil as proposed by Nishimura (1999). The various quantities of the solid and fluid phases are denoted by subscripts s and f .

(1) Rate-type equation of motion based on u - p formulation for saturated soil.

The following equation of motion is obtained for a saturated soil through u - p formulation.

$$\rho \dot{\mathbf{v}}_s = \operatorname{div} \mathbf{T} + \rho \mathbf{b} \quad (\text{A10})$$

Here, \mathbf{T} is the total Cauchy stress tensor (tension: positive), and \mathbf{b} is the body force vector per unit mass, which is assumed to be a constant vector. The superscript “\” on a variable expresses the material time derivative of the phase that is denoted by the subscript of the same variable. In Eq. (A10), ρ is the density of the saturated soil and is represented by the equation:

$$\rho = (1 - n)\rho^s + n\rho^f, n = \frac{v-1}{v} = \frac{e}{1+e} \quad (\text{A11})$$

where ρ^s and ρ^f are the respective densities of the soil particles and pore water when they exist singly, and n is the porosity. Furthermore, n can be expressed as a function of the specific volume v or the void ratio e as shown above.

Next, since the constitutive equation for a soil skeleton is an increment-type equation and the finite deformation analysis is carried out based on an updated Lagrangian scheme, we derive the rate-type equation of motion for a mixture (saturated soil) viewed from the solid phase.

$$\rho \ddot{\mathbf{v}}_s + \{nD_s\rho^f + \rho^f(\operatorname{tr} \mathbf{D}_s)\}(\dot{\mathbf{v}}_s - \mathbf{b}) = \operatorname{div} D_s \mathbf{S}_t, D_s \mathbf{S}_t = D_s \mathbf{T} + (\operatorname{tr} \mathbf{D}_s) \mathbf{T} - \mathbf{T} \mathbf{L}_s^T \quad (\text{A12})$$

In the above equation, which conforms to the method of expression used by Yatomi et al. (1989), D_s is the material time derivative viewed from the solid phase, and $D_s \mathbf{S}_t$ is the nominal stress rate viewed from the solid phase. \mathbf{L}_s and \mathbf{D}_s are the velocity gradient tensor and stretching tensor, respectively, of the solid phase and are defined later in the section that describes the compatibility conditions. The superscript “T” denotes transpose operation.

(2) Soil skeleton - water coupled equations:

(2-1) Continuity equation for saturated soil

Assuming that the soil particles and pore water are not compressible, the following equation is obtained as the continuity equation for saturated soils by using the sum of the mass conservation equation of each phase:

$$\operatorname{div} \mathbf{v}_s + \operatorname{div}\{n(\mathbf{v}_f - \mathbf{v}_s)\} = -\frac{n}{\rho^f} D_f \rho^f \quad (\text{A13})$$

where $n(\mathbf{v}_f - \mathbf{v}_s)$ is the average flow velocity of the pore water with respect to the soil skeleton.

(2-2) Average flow velocity equation for pore water, (so-called the generalized Darcy Law)

Assuming that the motion of the liquid phase is isotropic, the average flow velocity of pore water can be expressed by:

$$n(\mathbf{v}_f - \mathbf{v}_s) = -\frac{k}{\gamma_w} (\operatorname{grad} u - \rho^f \mathbf{b}) - \mathbf{v}_s \times \frac{\rho^f k}{\gamma_w} \quad (\text{A14})$$

where k is the permeability coefficient, $\gamma_w = \rho^f g$ is the weight of a unit volume of water, and g is the acceleration due to gravity. In deriving the above equation, the fundamental assumptions made for the u - p formulation have been used. As a result, the second term on the right-hand side of Eq. (A14) contains the acceleration term of the solid phase. The equation obtained by introducing Eq. (A14) into Eq. (A13) can be coupled with the rate type equation of motion for saturated soil [Eq. (A12)].



(3) *Principle of effective stresses:*

The equation below is obtained by following the Terzaghi's principle of effective stresses, where \mathbf{T}' is the Cauchy effective stress (tension: positive), u is the pore water pressure (compression: positive), and \mathbf{I} is the identity tensor.

$$\mathbf{T} = \mathbf{T}' - u\mathbf{I} \quad (\text{A15})$$

(4) *Constitutive equation of the soil skeleton:*

We employ the SYS Cam-clay model (Asaoka et al. (2002) described in the previous appendix for the constitutive equation of the soil skeleton as the linear relationship between \mathbf{T}' and \mathbf{D} :

$$\dot{\mathbf{T}'} = L[\mathbf{D}], \quad \dot{\mathbf{T}} = D_s \mathbf{T}' + \mathbf{T}' \boldsymbol{\Omega} - \boldsymbol{\Omega} \mathbf{T}' \quad (\text{A16})$$

where, in this paper, $\dot{\mathbf{T}'}$ is Green-Nagdhi (1965)'s rate of \mathbf{T}' ; $\boldsymbol{\Omega}$ is material spin tensor of the solid phase, expressed by $\boldsymbol{\Omega} = D_s \mathbf{R} \mathbf{R}^T$; and \mathbf{R} is the rotational tensor, derived from the deformation gradient tensor of the solid phase.

(5) *Compatibility condition:*

The definitions of the velocity gradient tensor \mathbf{L} and the stretching tensor \mathbf{D} of the solid phase are shown here.

$$\mathbf{L} = \frac{\partial \mathbf{v}_s}{\partial \mathbf{x}}, \quad \mathbf{D} = \frac{1}{2}(\mathbf{L} + \mathbf{L}^T) \quad (\text{A17})$$

(8) *Boundary conditions, initial conditions, and method of solution:*

The equations can be solved by allotting the boundary and initial conditions. In the actual case, the weak form of Eq. (A12) is used, and finite element discretization is carried out. By applying an extension (Asaoka et al., 1994; Asaoka et al., 1998a; Noda et al., 2008) of the method of Christian (1968) and Akai and Tamura (1978) to the equation obtained by substituting Eq. (A14) into Eq. (A13), we obtain a third order differential equation regarding the spatial coordinates and pore water pressure. To solve this equation, calculations are carried out by applying the linear acceleration method on the assumption that the jerk term varies linearly in place of acceleration and by performing implicit time integration. Furthermore, since there are many non-linear terms, iterative treatment is carried out for each time step.

REFERENCES

Akai, K., and Tamura, T. (1978). "Numerical analysis of multi-dimensional consolidation accompanied with elasto-plastic constitutive equation." *Proc. the Japan Society of Civil Engineers*, 269, 95-104. (in Japanese)

Asaoka, A., Nakano, M., and Noda, T. (1994). "Soil-water coupled behaviour of saturated clay near/at critical state." *Soils and Foundations*, 34(1), 91-106.

Asaoka, A., Nakano, M., Fernando, G.S.K., and Nozu, M. (1995). "Mass permeability concept in the analysis of treated ground with drains." *Soils and Foundations*, 35(3), 43-53.

Asaoka, A., Noda, T., and Fernando, G. S. K. (1997). "Effects of changes in geometry on the linear elastic consolidation deformation." *Soils and Foundations*, 37(1), 29-39.

Asaoka, A., Noda, T., and Kaneda, K. (1998a). "Displacement/traction boundary conditions represented by constraint conditions on velocity field of soil." *Soils and Foundations*, 38(4), 173-181.

Asaoka, A., Nakano, M., and Noda, T. (1998b). "Superloading yield surface concept for the saturated structured soils." *Proc. of 4th European Conference on Numerical Methods in Geotechnical Engineering*, 233-242.

Asaoka, A., Nakano, M., and Noda, T. (2000). "Superloading yield surface concept for highly structured soil behavior." *Soils and Foundations*, 40(2), 99-110.

Asaoka, A., Noda, T., Yamada, E., Kaneda, K., and Nakano, M. (2002). "An elasto-plastic description of two distinct volume change mechanisms of soils." *Soils and Foundations*, 42(5), 47-57.

Asaoka, A., and Noda, T. (2007). "All soils all states all round geo-analysis integration." *Proc. International Workshop on Constitutive Modeling - Development, Implementation, Evaluation, and Application*, Hong Kong, China, 11-27.

Association of vacuum consolidation technology (2013). “Technological material: Koushinku N&H method–Vacuum consolidation method, kairyogata”.

Atkinson, J.H., and Bransby P.L. (1978). *The Mechanics of Soil: An Introduction to Critical State Soil Mechanics*, McGraw-Hill Book Company (UK) Limited, Maidenhead, Berkshire, England, ISBN 07 084135 7.

Christian, J. T. (1968). “Undrained stress distribution by numerical method.” *Journal of Soil Mechanics & Foundations Division, ASCE*, 94(6), 1333-1345.

Green, A.E., and Naghdi, P.M. (1965). “A general theory of an elastic-plastic continuum.” *Archive for Rational Mechanics and Analysis*, 18(4), 251-281.

Hashiguchi K. (1978). “Plastic constitutive equations of granular materials.” *Proc. US-Japan Seminar on Continuum Mechanics and Statistical Approaches in the Mechanics of Granular Materials*, 321-329.

Hashiguchi, K. (1989). “Subloading surface model in unconventional plasticity.” *International Journal of Solids and Structures*, 25, 917-945.

Inagaki, M., Nakano, M., Noda, T., Tashiro, M., and Asaoka, A. (2010). “Proposal of a simple method for judging naturally deposited clay grounds exhibiting large long-term settlement due to embankment loading.” *Soils and Foundations*, 50(1), 109-122.

Japan Highway Public Corporation. (2005). “Design standards (Sekkei youryou), earthworks-countermeasures for soft ground” (in Japanese).

Mikasa, M. (1962). “On the significance of concept of structure in soil.” *Proc. 17th Annual Conference of JSCE*, 35-38 (in Japanese).

Nguyen, H. S., Tashiro, M., Inagaki, M., Yamada S., and Noda, T. (2015). “Simulation and evaluation of improvement effects by vertical drains/vacuum consolidation on peat ground under embankment loading based on a macro-element method with water absorption and discharge functions.” *Soils and Foundations*, 55(5), 1044-1057.

Nishimura, N. (1999). *Chapter 3 Soil Mechanics*, Handbook of Geotechnical Engineering, 51-64. (in Japanese)

Nippon Expressway Corporation (2015). *Design Standards (Sekkei youryou)*, Earthworks-Countermeasures for Soft Ground (in Japanese).

Noda, T., Asaoka, A., Nakano, M., Yamada, E., and Tashiro M. (2005). “Progressive consolidation settlement of naturally deposited clayey soil under embankment loading.” *Soils and Foundations*, 45(5), 39-51.

Noda, T., Asaoka, A., and Nakano, M. (2008). “Soil-water coupled finite deformation analysis based on a rate-type equation of motion incorporating the SYS Cam-clay model.” *Soils and Foundations*, 48(6), 771-790.

Noda, T., Takeuchi, H., Nakai, K., and Asaoka, A. (2009). “Co-seismic and post-seismic behavior of an alternately layered sand-clay ground and embankment system accompanied by soil disturbance.” *Soils and Foundations*, 49(5), 739-756.

Roscoe, K. H., and Burland, J. B. (1968). *On the generalized stress-strain behaviour of 'wet' clay*, Engineering Plasticity, Cambridge University Press, 535-609.

Sekiguchi H., and Ohta H. (1977). “Induced anisotropy and time dependency in clays, Constitutive Equations of Soils.” *Proc. 9th Int. Conf. Soil Mech. Found. Eng., Specialty Session 9*, 229-238.

Sekiguchi, H., Shibata, T., Fujimoto, A., and Yamaguchi, H. (1986). “A macro-element approach to analyzing the plane-strain behavior of soft foundation with vertical drains.” *Proc. 31st Symposium of JGS*, 111-116 (in Japanese).

Tashiro, M., Noda, T., Inagaki, M., Nakano, M., and Asaoka, A. (2011). “Prediction of settlement in natural deposited clay ground with risk of large residual settlement due to embankment loading.” *Soils and Foundations*, 51(1), 133-149.

Tashiro, M., Nguyen, H. S., Inagaki, M., Yamada, S., and Noda, T. (2015). “Simulation of large-scale deformation of ultra-soft peaty ground under test embankment loading and investigation of effective countermeasures against residual settlement and failure.” *Soils and Foundations*, 55(2), 343-358.

Terzaghi, K. (1925) *Erdbaumechanik auf Bodenphysikalischen Grundlagen*, Deuticke, Wien.

Yamada, S., Noda, T., Tashiro, M., and Nguyen H. S. (2015). “Macro element method with water absorption and discharge functions for vertical drains.” *Soils and Foundations*, 55(5), 1113-1128.

Yatomi, C., Yashima, A., Iizuka, A., and Sano, I. (1989). “General theory of shear bands formation by a non-coaxial Cam-clay model.” *Soils and Foundations*, 29(3), 41-53.



INTERNATIONAL JOURNAL OF
**GEOENGINEERING
CASE HISTORIES**

*The Journal's Open Access Mission is
generously supported by the following Organizations:*



Geosyntec
consultants

engineers | scientists | innovators

CONETEC



ENGEO
Expect Excellence

Access the content of the ISSMGE International Journal of Geoengineering Case Histories at:
<https://www.geocasehistoriesjournal.org>